frontiers in Materials

ORIGINAL RESEARCH
published: 21 May 2020
doi: 10.3389/fmats.2020.00130

Thermal, Mechanical and Micromechanical Analysis of PLA/PBAT/POE-g-GMA Extruded Ternary Blends

*Laura Aliotta[1], Vito Gigante[1], Oriana Acucella[1], Francesca Signori[1,2] and Andrea Lazzeri[1,2]**

[1] DICI-Department of Civil and Industrial Engineering, University of Pisa, Pisa, Italy, [2] IPCF-CNR, Area della Ricerca di Pisa, Pisa, Italy

In order to toughen Poly(lactic) acid and binary blends with low PBAT content while maintaining a high biodegradability of the final material, poly(lactic) acid (PLA)/poly(butylene-adipate-co-terephthalate) (PBAT)/ polyolefin elastomer grafted with glycidyl methacrylate (POE-g-GMA) extruded ternary blends have been investigated in this work from a thermal, mechanical, and rheological point of view. The two elastomers have been added in different amounts as dispersed phases into the PLA matrix, paying attention to the final objective: the design of a 90% biodegradable formulation according to EN 13432. These ternary blends exhibited improved impact properties but still low elongation at break. Consequently, to the ternary composition with the best compromise of PLA quantity, biodegradability and thermo-mechanical properties (81 wt.% PLA, 9 wt.% PBAT, and 10 wt.% POE-g-GMA) a small quantity (10 wt.%) of a biobased plasticizer was added in order to further increase the impact properties in parallel with the tensile flexibility. Two types of plasticizers were investigated, one not reactive [Acetyl Tributyl Citrate (ATBC)], and one reactive [Glycidyl ether (EJ-400)]. A micromechanical study, in order to investigate the toughening mechanism of these systems, was carried out on the final formulations. They were also examined by dilatometric tests and elasto-plastic fracture mechanics correlating the data obtained to the morphology and to the rheological properties. In conclusion, the best compromise between impact, tensile properties and biodegradability content was achieved using the reactive plasticizer (EJ-400) whose interaction with the matrix is confirmed by the FT-IR analysis.

Keywords: rubber toughening, poly(lactic) acid, biodegradable polymers, ternary blends, mechanical properties

OPEN ACCESS

Edited by:
Luca Valentini,
University of Perugia, Italy

Reviewed by:
Micaela Degli Esposti,
University of Bologna, Italy
Leire Ruiz Rubio,
University of the Basque Country, Spain

***Correspondence:**
Andrea Lazzeri
andrea.lazzeri@unipi.it;
a.lazzeri@ing.unipi.it

Specialty section:
This article was submitted to Polymeric and Composite Materials, a section of the journal Frontiers in Materials

Received: *09 October 2019*
Accepted: *20 April 2020*
Published: *21 May 2020*

Citation:
Aliotta L, Gigante V, Acucella O, Signori F and Lazzeri A (2020) Thermal, Mechanical and Micromechanical Analysis of PLA/PBAT/POE-g-GMA Extruded Ternary Blends. Front. Mater. 7:130. doi: 10.3389/fmats.2020.00130

INTRODUCTION

Several and important qualities for everyday life, associated to low processing costs, make plastics fundamental in different sectors. About 150 million tons of plastics are used everywhere and its consumption is expected to grow up in the next years (La Mantia et al., 2017; Cinelli et al., 2019). Nevertheless, the society is acquiring a new awareness to adapt the third millennium consumerist and technological needs to the respect of the environment and of the human health. At this purpose, investigation on biodegradable polymers is of fundamental importance. The resistance of polymeric materials to chemical, physical and biological degradation has become a crucial problem and wastes are not acceptable. A possible alternative to classical polymers can be biodegradable polymers

(biobased and not) that fulfill the conditions of biodegradability, biocompatibility and release of low or null toxicity. Nowadays, these biodegradable polymers can be the solution to overcome the effect of plastic wastes on the environment caused by the limited disposal methods. Differently to bio-based polymers, derived partially or completely from renewable resources, biodegradable polymers are not determined by the origin of the raw material. According to the biodegradability definition: "a given substance can be completely converted into water, CO_2, and biomass through the action of microorganisms such as fungi and bacteria" (Platt, 2006). This property does not depend on the origin of the raw materials, but it depends just from the chemical composition. Biodegradability is a certified characteristic (European Committee for Standardisation, 1999). In according to EN 13432 norm: "the polymer must be converted to CO_2 (by over 90%) within 180 days under specific conditions of temperature, humidity, and oxygen level." (Künkel et al., 2016). In many fields, biodegradability gives to a product an additional value.

Among of all biodegradable polymers, poly(lactic acid) (PLA), that is fully biobased, shows very good mechanical properties, complete renewability and low production cost if compared to other biodegradable polymers (Gross and Kalra, 2002). Nevertheless, processing drawbacks, brittleness, slow crystallization rate, poor toughness and limited thermal resistance (due to its glass transition temperature around 60°C) limit the use of PLA in several markets (Barletta and Puopolo, 2019). Physical performance of PLA can be improved through numerous methods including copolymerization (Anderson et al., 2008; Phuong et al., 2014), plasticization (Baiardo et al., 2003; Coltelli et al., 2008), rubber toughening (Su et al., 2009; Gigante et al., 2019), rigid filler toughening (Murariu and Dubois, 2016; Aliotta et al., 2019), and physical blending (Zhang et al., 2014; Sedničková et al., 2018).

However, PLA brittleness is the main drawback, in order to improve PLA toughness and flexibility, binary blends of PLA with other ductile polymers have been widely reported; remarkably, less literature is present about multiphase blends, in particular ternary plasticized blends. Some interesting results have been reported for PLA-based multicomponent blends having significant improvement in mechanical properties (Anderson and Hillmyer, 2004; Grande and Carvalho, 2011; Kunthadong et al., 2015; Nagarajan et al., 2018). Sarazin et al. (2008) evaluated ternary blends with PLA, polycaprolactone (PCL), and termoplastic starch (TPS) (Sarazin et al., 2008). They showed that adding PCL to PLA/TPS binary blends, the tensile ductility increases; consequently to reach brilliant combined performances, blending PLA/TPS with another flexible polymer could be an useful method. Ren et al. (2009) instead, stated that biodegradable ternary blends of TPS, PLA and Poly(butylene adipate-co-terephthalate) (PBAT) give good impact resistance when a low content of compatibilizer (an anhydride functionalized polyester) is added.

On the basis of these evidences, in this work, the impact resistance of PLA was improved using a ternary blend approach without compromising the end of life biodegradability (following the EN 13432 standard). Small amounts of PBAT and a polyolefin elastomer grafted with Glycidyl Methacrylate (POE-g-GMA) were added as dispersed phase into PLA matrix.

The idea adopted in this work was to use PBAT, coupled with POE-g-GMA, to reach a good compromise between an acceptable increment of impact resistance (thanks to POE-g-GMA) and, at the same time, a noteworthy improvement in tensile flexibility (thanks to PBAT).

It is known that PLA/PBAT binary blends (from until 20 wt.% of PBAT content), processed via melt blending in a twin screw extruder, lead to a well dispersed systems of PBAT particles into the PLA matrix (Jiang et al., 2006; Hamad et al., 2018). This morphology is attributable to the high immiscibility between the two polymers, that depends to their different solubility parameters [PLA $\sim$ 10.1 $(cal/cm^3)^{1/2}$ and PBAT $\sim$ 22.95 $(cal/cm^3)^{1/2}$] and it causes a weak interfacial adhesion between the two phases (Kumar et al., 2010). Furthermore, the addition of PBAT changes the melt rheology increasing the melt processability window (Gu et al., 2008). From a mechanical point of view, PBAT improves the ductility of PLA without compromising, in an evident way, its strength. Until the 2.5 wt.% PBAT content, the ductile fracture of PLA/PBAT binary blends form a compatible system (Yeh et al., 2009).

Glycidyl methacrylate (GMA) grafted polyolefin elastomers (POE) are often used in polyester blends (Hu et al., 1996; Forghani et al., 2018). Consequently, as PLA shows a good chemical functionality (Sun et al., 2011) it can be combined with POE-g-GMA. It has been stated that epoxy groups react with carboxyl or hydroxyl groups of polyesters, the end hydroxyl and/or carboxyl groups of PLA react with epoxy groups of POE-g-GMA via nucleophilic substitution under appropriate extrusion conditions. For this reason, with PLA/POE-g-GMA blends, a large toughening effect can be expected if a *in-situ* copolymer at the interfaces could form during extrusion enabling a good particle matrix adhesion, a good dispersion and a small particles size of the rubbery phase (Su et al., 2009). Therefore, it will be expected that POE-g-GMA could have a significant toughening effect on PLA thanks to the possible reaction that can occur between the epoxy groups of POE-g-GMA and carboxyl end-groups of PLA.

To use the potentiality of these two already elastomers described (PBAT and POE-g-GMA), a compromise has to be found as far as concern concentration, morphology and resulting properties. First of all, it is necessary to conduct a first screening step to set the suitable composition; then an optimization of the best formulation can be made adding a plasticizer that improves the processability, the elongation at break and impact properties at room temperature (Plackett et al., 2003; Quero et al., 2012; Mallegni et al., 2018).

In this work, a detailed study has been conducted, in fact a rheological, thermal, mechanichal and morphological characterization has been carried out on semi-industrial extruded ternary blends of PLA/PBAT/POE-g-GMA. At the best composition, small amounts of two different biodegradable plasticizers [Acetyl Tributyl Citrate (ATBC) (not reactive) and Glycidyl ether (EJ-400, reactive)] were added. A study of the micromechanical deformation processes was carried out on the best ternary blends where the parallel growth

of the impact strength and of the tensile ductility could be observed. In particular, the effect of the plasticizer addition was deeply investigated also through the FT-IR analysis of the chemical bonds formed as a result of mutual interaction. Thanks to the use of a videoextensometer capable to register both axial and trasversal elongation it was possible to register the volume variation and correlate the volume increment to the micormechanichal deformation processes (debonding, cavitation, voids growth. . .). Also the capability of the plasticized ternary blends to absorb energy at slow rate was investigated by the elasto-plastic fracture mechanics approach based on the ESIS load separation criterion.

MATERIALS AND METHODS

Materials (Chemicals)

The materials used for this work (data taken from technical datasheets) were:

- PLA2003D purchased from NatureWorks (thermoforming and extrusion grade), [melt flow index (MFI): 6 g/10 min (210°C, 2.16 kg), nominal average molar mass: 200,000 g/mol, density: 1.24 g/cm^3]. It contains about 4% of D-lactic acid units to lower the melting point and the crystallization tendency improving the processability during the melting extrusion.
- PBAT: Ecoflex C1200 purchased from BASF. It is a biodegradable, random aliphatic-aromatic copolyester based on the monomers 1.4-butanediol, adipic acid and terephthalic acid, [MFI: 2.7–5 g/10 min (190°C, 2.16 kg), nominal average molar mass: 126,000 g/mol, density 1.26 g/cm^3].
- POE-g-GMA: trade name SOG2, purchased from Fine-blend Compatibilizer Jiangsu Co., Ltd. [MFI: 2–5 g/10 min (190°C, 2.16 kg), nominal average molar mass: 220,000 g/mol, density of 0.88 g/cm^3, and grafted ratio of 0.8–1.2 wt%].
- ATBC from Tecnosintesi S.p.A. was used as not reactive plasticizer. ATBC is prepared by the acetylation of tributylcitrate and it appears as a colorless liquid largely used with PLA (Maiza et al., 2016) [density: 1.05 g/cm^3, molecular weight: 402.5 g/mol].
- Glyether Resin (EJ-400) from Jsi Co., Ltd., was used as reactive plasticizer that it would act both as plasticizer and compatibilizer [density 1.21 g/cm^3, molecular weight: 305 g/eq].

Blends and Specimens' Preparation

Binary and ternary blends with different compositions (**Table 1**), containing as dispersed phases in PLA matrix different amounts of PBAT alone or PBAT and POE-g-GMA, were extruded with a semi-industrial COMAC EBC 25HT twin screw extruder (L/D = 44) to achieve granules of about 2 mm diameter. After the evaluation of the ternary blends containing the best compromise between PLA quantity, biodegradability and mechanical properties, comparing them with pure PLA and binary blends PLA/PBAT, the effect of the addition of two different plasticizers (ATBC and EJ-400) was evaluated. Before the extrusion, all solid materials were dried in a ventilated oven for at least 24 h. PLA and PBAT were introduced into the main extruder feeder. POE-g-GMA, was fed, separately, from a specific feeder which allows, fixed the weight percentage to be added, a constant concentration in the melt during the extrusion. The plasticizers were introduced by the use of a peristaltic pump (Verderflex–Vantage 3000) suitably calibrated to guarantee a constant flow rate maintaining the fixed plasticizing concentration. During the extrusion, the temperature profile in the zones from 1 to 11 was: 150/180/180/180/185/185/185/185/170/165/150°C, with the die zone at 150°C. The screw rate was 260 rpm. The extruded filaments were cooled in a water bath at room temperature and reduced in pellets by an automatic cutter. All pellets were finally dried in a Piovan DP 604-615 dryer at 60°C.

After the extrusion, pelletized binary and ternary blends were molded using a Megatech H10/18 injection molding machine to obtain dog-bone (Haake Type 3) and parallelepiped Charpy specimens (ISO179). The operative conditions of injection molding process are reported in **Table 2**.

Torque Characterization

An indirect measurement of the viscosity during the extrusion can be obtained through torque measurements. These measures were performed on 6 g of melt pellets by using a MiniLab II

TABLE 1 | Blends name and compositions.

	Mass composition (%)				
Blend name	**PLA**	**PBAT**	**POE-g-GMA**	**ATBC**	**EJ**
PLA	100	0	0	0	0
95-5	95	5	0	0	0
90-10	90	10	0	0	0
(95-5)+10POE	85.5	4.5	10	0	0
(95-5)+15POE	80.75	4.25	15	0	0
(95-5)+20POE	76	4	20	0	0
(90-10)+10POE	81	9	10	0	0
(90-10)+15POE	76.5	8.5	15	0	0
(90-10)+20POE	72	8	20	0	0
(90-10-10)+10ATBC	72.9	8.1	9	10	10
(90-10-10)+10EJ	72.9	8.1	9	10	10

TABLE 2 | Injection molding conditions.

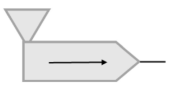	**Binary and ternary blends**	**Plasticized ternary blends**
Temperature profile from feeder to the injection zone (°C)	175 / 180 / 185	170 / 165 / 160
Mold Temperature (°C)	50	40
Injection Holding Time (s)	10	15
Cooling Time (s)	10–15	15
Injection Pressure (bar)	100	90

Haake^{TM} twin-screw microcompounder, equipped with conical screws, at 180°C and 100 rpm. The extrusion was monitored for 1 min and every 10 s an assessment of the torque value was recorded. The measurements were carried out three times and the average value was reported.

Mechanical Characterization

For tensile and dilatometry tests Haake Type 3 dog-bone tensile bars (width: 5 mm, length: 25 mm, thickness 1.5 mm) were used. Tensile tests were carried out, at room temperature, at a crosshead speed of 10 mm/min on an MTS Criterion model 43 universal tensile testing machine equipped with a 10 kN load cell and interfaced with a computer running MTS Elite Software. Tests were conducted not before 24 h from specimen injection molding. At least ten specimens were tested for each blend and the average values were reported.

Tensile dilatometry tests were also carried out with MTS universal tensile testing machine at a crosshead speed of 10 mm/min. Given the large quantity of blends prepared, dilatometry tests were carried out only for the best compositions. At least five samples for each selected material were tested at room temperature. Transversal and axial specimen elongations were recorded, during tensile test, using a video extensometer (GenieHM1024 Teledyne DALSA camera) interfaced with a computer running ProVis software (Fundamental Video Extensometer); the data in real-time were then transferred to MTS Elite software in order to measure not only the axial and transversal strains but also the load value. The two lateral strain components were assumed to be equal and the volume strain was calculated using the following equation (Lazzeri et al., 2004; Aliotta et al., 2019):

$$\frac{\Delta V}{V_0} = (1+\varepsilon_1)(1+\varepsilon_2)^2 - 1 \tag{1}$$

where ΔV is the change in volume, V_0 the original volume, ε_1 the longitudinal (or axial) strain, and ε_2 the lateral strain.

Impact tests were performed on V-notched specimens (width:10 mm, length:80 mm, thickness: 4 mm, V-notch 2 mm at 45°) using a 15 J Charpy pendulum of an Instron CEAST 9050. The standard method ISO179:2000 was followed. For each blend, at least ten specimens, at room temperature, were tested.

Three-point bending tests were carried out, on the best blends, to evaluate the energy accumulated by the sample before the fracture with the already cited MTS universal testing machine. The methodology used to calculate fracture energy at the starting point of crack propagation (J_{Ilim}) follows the ESIS TC4 load separation protocol (Bernal et al., 1996; Baldi et al., 2013). According to this protocol, the tests must to be carried out at 1 mm/min crosshead speed on 80 × 10 × 4 mm SENB specimens cut in two different ways: "*sharp*" (half notched samples) and "*blunt*" (drilled in the center with a 2 mm diameter hole and then cut for half width). The sharp notch (5 mm) was achieved using compressed air during the cutting process to limit the "*notch closing*" material phenomenon due to overheating caused by the cutter. A manual cutter, used as a broaching machine through the rapid entry and exit of the blade from the specimen, was manipulated obtaining a notch without plastic deformation or heating due to the passage of the blade. A "*sacrificial specimen*" placed under the "*good one*" was used to guarantee a correct notch of the sample without closure (qualitatively evaluated with a "passing" paper) and avoiding plastic deformation around to it. At least five specimens were tested for each selected blends.

The J_{lim} value has been calculated following the Load Separation Criterion (Sharobeam and Landes, 1991). This procedure (Baldi et al., 2010, 2013; Agnelli et al., 2012; Blackman et al., 2015) is based on the construction of the load separation parameter curve, obtained from the load P vs. displacement u in the three-point bending tests. The curves were recorded for the two types of specimens (*sharp* and *blunt*). In the sharp specimens the fracture propagation occurs, whereas in the blunt the crack growth does not occur (only plastic deformation occurs).

The S_{sb} curve (Equation 2) represents the variation of load separation parameter and it is defined as:

$$S_{sb} = \frac{P_s}{P_b}|u_{pl} \tag{2}$$

where s and b indicate the sharp and the blunt notched specimens, respectively. The plastic displacement u_{pl}, instead, is expressed as:

$$u_{pl} = u - P \cdot C_0 \tag{3}$$

where u is the total displacement and C_0 is the initial elastic specimen compliance. Baldi et al. (Baldi et al., 2013; Agnelli et al., 2018) noticed that fracture initiation can be a complex progressive process for ductile polymers, characterized by the slow development of the crack front across the thickness of fracture transition. This limit point represents a pseudo-initiation of fracture. Defined the limit point, the corresponding J_{lim} can be evaluated by Equation 4:

$$J_{lim} = \frac{2 \cdot U_{lim}}{b \cdot (w - a_0)} \tag{4}$$

where U_{lim} is the elastic behavior limit point, b is the sample thickness, w is the sample width and a_0 is the initial crack length.

FT-IR Characterization

ATR spectra were recorded on rectangular Charpy specimens, at room temperature in the 400–4000 cm^{-1} range, by means of a Nicolet 380 FT-IR spectrometer equipped with a smart iTX ATR accessory. The 1700–1800 cm^{-1} range was investigated in details, to evaluate whether a shift of the ester carbonyl stretching absorption peak occurred as a consequence of the addition of POE-g-GMA on 90/10 PLA/PBAT blends and as a consequence of the addition of ATBC and EJ-400 on ternary blends. This behavior would indicate the presence of physical interactions among PLA matrix and the additives.

Thermal Characterization

Thermal properties were investigated by calorimetric analysis using a Q200 TA-Instrument differential scanning calorimeter (DSC) equipped with a RSC cooling system. Nitrogen, set at 50 mL/min, was used as purge gas for all measurements. Indium was adopted as a standard for temperature and enthalpy

calibration of DSC. The materials used for DSC analysis were cut from the dog-bone injection molding specimens. The sampling was carried out exactly in the same region of the injection molded specimens to avoid differences ascribable to different cooling rates in the specimen thickness. Aluminum pans with samples were sealed before measurement and the mass of the samples used varied between 10 and 15 mg. The samples were heated from room temperature at 10°C/min to 200°C under a nitrogen atmosphere and held for 5 min to remove the previous thermal history. Then, the samples were cooled at 10°C/min to −50°C and held for 5 min then they were heated again at 10°C/min to 200°C to record the crystallization and melting behaviors.

Melting temperature (T_m) and the cold crystallization temperature (T_{cc}) of the blends were recorded at the maximum of the melting peak and at the minimum of the cold crystallization peak, respectively. The enthalpies of melting (ΔH_m) and cold crystallization (ΔH_{cc}) were determined from the corresponding peak areas in the second heating thermograms. The crystallinity percentage (X_{cc}) of PLA and its blends was calculated as follows:

$$X_{cc(PLA)} = \frac{\Delta H_{m(PLA)} - \Delta H_{cc(PLA)}}{\Delta H^{\circ}_{m(PLA)} wt._{PLA}} \cdot 100 \quad (5)$$

where $\Delta H_{m(PLA)}$ is the melting enthalpy of PLA, $\Delta H_{cc(PLA)}$ is the cold crystallization enthalpy of PLA, and $\Delta H^{\circ}{}_{m(PLA)}$ is the melting enthalpy of 100% crystalline PLA that is 93 J/g (Wang et al., 2018), $wt_{(PLA)}$ is the weight fraction of PLA in the blends.

Morphological Characterization

In order to investigate the morphology of the best ternary systems, the cryogenic fractured cross-sections of the Charpy samples were analyzed, after gold sputtering, by a FEI Quanta 450 FEG scanning electron microscope (SEM) (magnifications 4000x for **Figure 3** and 500x for **Figure 9**) equipped with a Large Field Detector for low kV imaging simultaneous secondary electron (SE).

The fracture surface of specimens broken during tensile test offers the best reliable information about the deformation mechanism. Consequently, to study and to better clarify the micromechanics deformation, after the tensile test some specimens have been cold fractured along the tensile direction. The specimens were coated, by using a sputter coater Edward S150B, with a thin layer of gold prior to microscopy to avoid charge build up.

RESULTS AND DISCUSSION

First Screening on Binary and Ternary Blends

The first methods used to evaluate the feasibility of ternary blends composition were the uniaxial static tensile test and the Charpy impact test. A comparison between ternary PLA/PBAT/POE-g-GMA ternary blends and pure PLA and PLA/PBAT binary blends was carried out. The basis from which this work started (a binary blend with 5 and 10% of PBAT dispersed into the PLA matrix) was substantiated by a double reason: not increase the petro-quantity, although biodegradable, of the entire formulation and to evaluate the processes of toughening and increase of ductility with the addition of the two elastomers but always within a continuous PLA matrix. The addition of POE-g-GMA was of 10, 15, and 20 wt.% on the two starting binary blends (readjusting the formulations in such a way that the mass composition can be 100%).

For the ternary blends, the results of tensile tests (**Table 3** and **Figure 1**) showed a decrement of Young's modulus increasing the rubber content. Despite of the elastomer addition, the elongation at break increases only slightly, and the ternary blends did not show a yielding point (as the pure PLA and the binary blends did). It is clear that 10 wt.%. of PBAT guarantees a substantial improvement in the elongation at break, which is lost with the addition of the third phase. However, the effect of POE-g-GMA is evident analyzing the **Figure 1D** in which 10 wt.% of polyolefin elastomer addition guarantees a Charpy impact strength value almost tripled compared to pure PLA and binary blends. This improvement in the Charpy Impact Resistance is remarkable if compared also to other binary PLA-PBAT systems reported in literature (Zhang et al., 2009).

The mechanical results indicate that these ternary blends show dissimilar deformation mechanisms when the loading conditions change (for example in tensile and impact tests). Tensile tests, indeed, are carried at slow rate while impact tests at higher rate (Zhang et al., 2014).

The torque trends of the pure materials (PLA, PBAT, and POE-g-GMA) and of the ternary blends are showed in **Figure 2**, in order to assess and study the melt strength during the extrusion. It can be observed that PLA showed a melt strength double respect to that of the materials used as dispersed phase. PBAT and POE-g-GMA were characterized by comparable torques, and consequently their processability was similar. For the (95-5) based ternary blends not significant torque changes were encountered increasing the POE-g-GMA content. On the other hand, for the (90-10) based ternary blends, viscosity decreases increasing the POE-g-GMA content, as previously reported for similar cases (Signori et al., 2009).

Figure 3A reports a SEM image of the (90-10)+10POE blend in which irregular platelets of POE-g-GMA and spherical particles of PBAT are dispersed separately into the PLA matrix. For ternary systems, in which there are two dispersed phases in a continuous matrix, like the systems studied in this work, two distinct types of phase morphology can be encountered. Dekkers et al. (1991) stated that one situation can be characterized by two dispersed phases in which one is encapsulated in the other (core–shell morphology). Alternatively, the two phases are dispersed separately into the matrix (Dekkers et al., 1991). The mechanical properties and the rheology of ternary blends are significantly affected by their morphology (Luzinov et al., 1999; Xue et al., 2018). Furthermore, it is important to underline which factors affect the phase structure of multicomponent blends. Viscosity of components [in linear proportionality with the torque (Gupta and Srinivasan, 1993)], composition and interfacial interaction between phases are the main factors that influence the morphology of ternary polymer blends (Utracki and Shi, 1992).

TABLE 3 | Mechanical results of tensile tests with experimental deviation.

Blend name	Elastic modulus (GPa)	Stress at break (MPa)	Elongation at break (%)	Yield stress (MPa)	Elongation at yield (%)	Charpy impact resistance (kJ/m^2)
PLA	3.2 ± 0.09	55.0 ± 1.00	2.5 ± 0.30	/	/	3.0 ± 0.31
95-5	3.1 ± 0.22	20.1 ± 1.22	6.4 ± 0.71	58.6 ± 2.10	4.6 ± 0.25	3.3 ± 0.23
90-10	2.7 ± 0.05	24.5 ± 0.75	12.4 ± 2.60	54.1 ± 1.80	4.8 ± 0.18	3.4 ± 0.10
(95-5)+10POE	2.8 ± 0.07	37.4 ± 2.09	4.4 ± 0.21	/	/	6.7 ± 1.01
(95-5)+15POE	2.5 ± 0.05	32.4 ± 0.87	3.9 ± 0.08	/	/	6.8 ± 0.61
(95-5)+20POE	2.1 ± 0.23	27.7 ± 0.19	4.5 ± 0.19	/	/	6.9 ± 0.92
(90-10)+10POE	2.1 ± 0.17	34.6 ± 1.03	4.4 ± 0.11	/	/	7.2 ± 0.93
(90-10)+15POE	2.1 ± 0.03	31.2 ± 1.69	4.4 ± 0.19	/	/	7.2 ± 0.94
(90-10)+20POE	1.6 ± 0.14	27.0 ± 0.13	4.4 ± 0.13	/	/	7.3 ± 0.44
(90-10-10)+10ATBC	1.2 ± 0.10	15.5 ± 0.70	13.8 ± 0.70	21.7 ± 0.91	4.5 ± 0.21	7.5 ± 0.15
(90-10-10)+10EJ	1.5 ± 0.22	18.9 ± 1.85	8.0 ± 0.90	22.8 ± 0.79	4.3 ± 0.79	9.1 ± 0.81

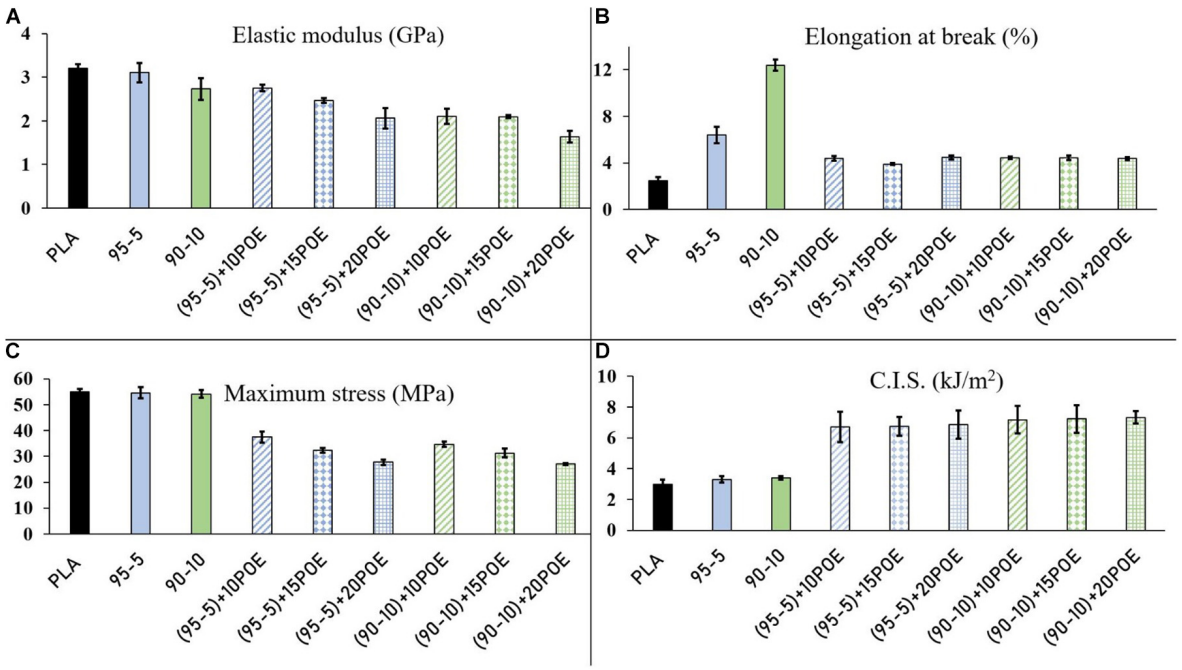

FIGURE 1 | Mechanical properties for PLA, binary blends and ternary blends: **(A)** Elastic Modulus; **(B)** Stress at break; **(C)** Elongation at break (%); **(D)** Charpy Impact Resistance.

The effect of interfacial tension between phases on the morphology for a ternary system (in which A is the continuous phase and B and C are the dispersed phases) can be evaluated by the spreading coefficient (λ_{BC} of the B-phase on the C-phase) defined as (Hemmati et al., 2001):

$$\lambda_{BC} = \gamma_{AC} - \gamma_{AB} - \gamma_{BC} \quad (6)$$

where γ_x are the interfacial tension for each component pair. If λ_{BC} is positive, the B-phase will encapsulate the C-phase. Similarly, for λ_{CB} the equation will be:

$$\lambda_{CB} = \gamma_{AB} - \gamma_{AC} - \gamma_{BC} \quad (7)$$

A core–shell morphology is characterized by a positive value of λ_{CB}; the C-phase will encapsulate the B-phase. On the other hand, both negative lambda values will return a dispersed system where the B and C phases are separated in the matrix. **Table 4** reports the lambda results for the ternary systems analyzed. The values of interfacial tensions were taken from literature (Wu, 1985; Nofar et al., 2015). It can be observed that both λ_{BC} and λ_{CB} are negative. This result means that PBAT and POE-g-GMA form two distinct dispersed phases in the PLA matrix. This morphology was indeed verified by SEM analysis (**Figure 3**).

Differential scanning calorimeter heating curves of PLA, PBAT, POE-g-GMA and ternary blends after crystallizing from melt are shown in **Figure 4**. The thermal properties of PLA and PBAT correspond to what is reported in literature (Cao et al., 2003; Al-Itry et al., 2012). PLA shows a glass transition temperature around 60°C, a cold crystallization temperature

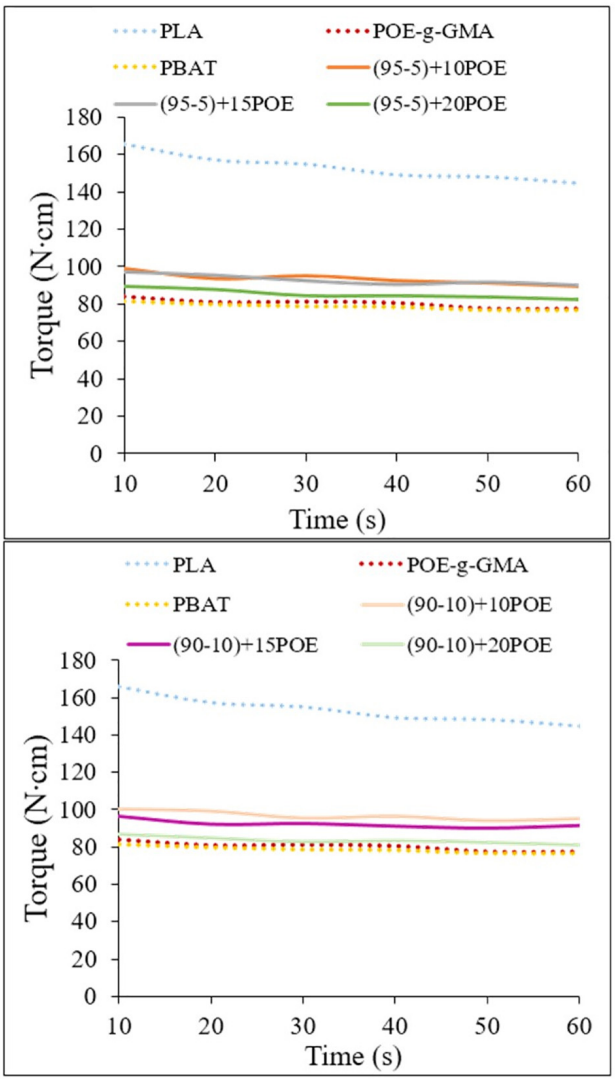

FIGURE 2 | Torque trends for pure polymers and differences with ternary blends.

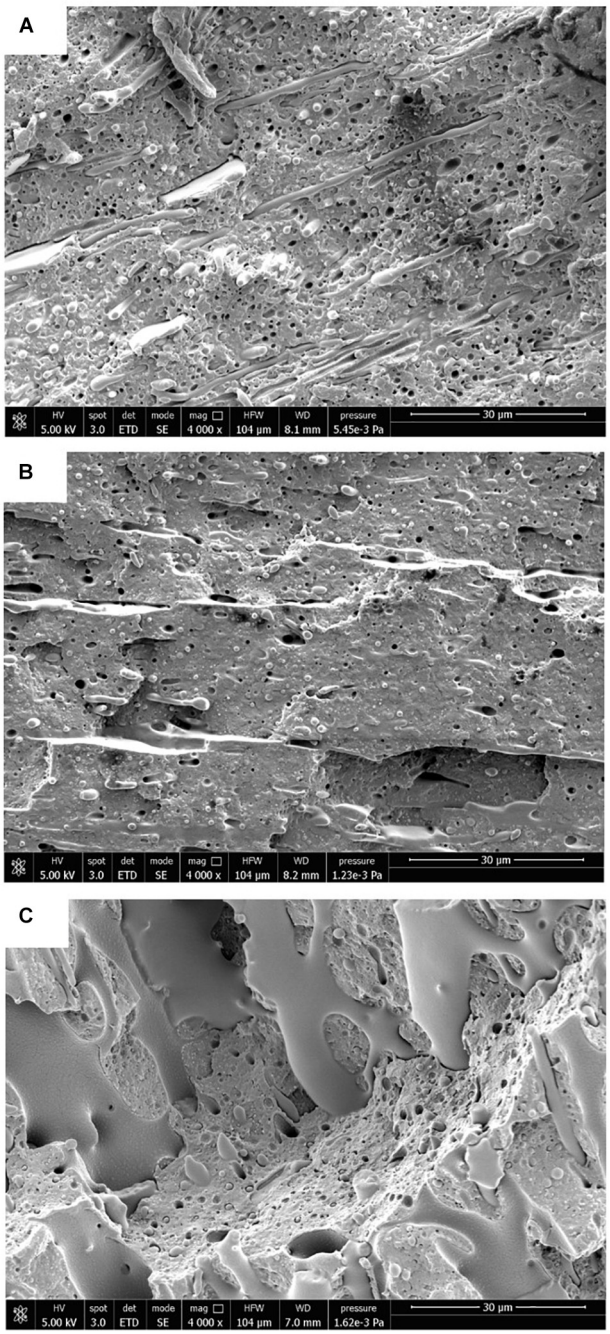

FIGURE 3 | SEM micrographs of plasticized ternary blends in comparison with (90-10)+10POE: **(A)** (90-10)+10POE; **(B)** (90-10-10)+10ATBC; **(C)** (90-10-10)+10EJ.

around 110°C and melting temperature around 150°C. The crystallization rate of PLA due to the presence of D-units is very low and, consequently, also the crystallinity content that it is around 3%. Concerning neat PBAT, its second heating scan showed a glass transition centered at around −35°C and a broad melting peak around 120°C consistent to what can be found in literature (Kumar et al., 2010).

In the thermogram of POE-g-GMA the glass transition temperature is not visible, according to datasheet and literature (Su et al., 2009) it must occur around −40°C. Two melting peaks are present in the POE-g-GMA thermogram. One melting peak at around 60°C degree that it is related to grafted polyethylene octane and another melting peak in correspondence of 160°C that it is typical of polypropylene. This melting behavior is typical of polyethylene octane rubber in which also traces of polypropylene are present (Svoboda et al., 2010).

Analyzing the ternary blends, it can be observed that increasing the content of POE-g-GMA, it does not affect either the glass transition or the melting peak. The cold crystallization temperature and the melting temperature of PLA decrease with the addition of PBAT and POE-g-GMA. It can be observed that in all ternary blends there is a large cold crystallization exothermal peak, the area of which is similar to that of the

TABLE 4 | Spreading coefficient and interfacial interaction for the PLA / PBAT/ POE-g-GMA system.

Material name	γ (180°C)	γ_p (180°C) (mN/m)	γ_d (180°C) (mN/m)	γ_{AB} (180°C) (mN/m)	γ_{AC} (180°C) (mN/m)	γ_{BC} (180°C) (mN/m)	λ_{CB} (mN/m)	λ_{BC} (mN/m)
A (PLA)	43	11.5	31.5	0.4	6.9	8.7	−15.26	−2.16
B (PBAT)	46	10	36					
C (POE-g-GMA)	30.7	8.6	22.1					

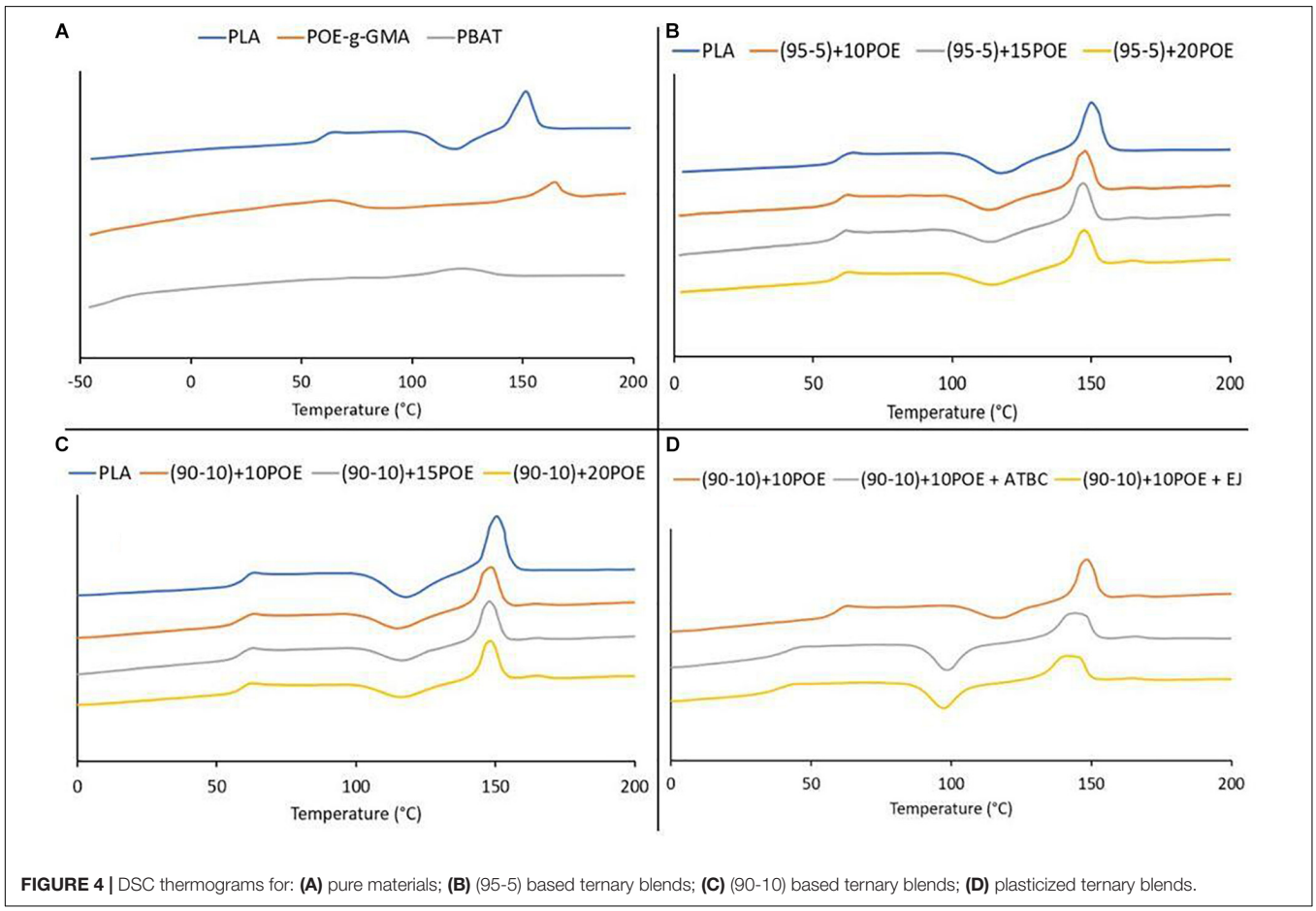

FIGURE 4 | DSC thermograms for: **(A)** pure materials; **(B)** (95-5) based ternary blends; **(C)** (90-10) based ternary blends; **(D)** plasticized ternary blends.

melting endotherm peak; this suggests that the PLA is almost in the amorphous state (Ishida et al., 2009) as confirmed by the PLA crystallinity content percentage reported in **Table 5**. However, the addition of PBAT and POE-g-GMA enables the crystallization ability of PLA encouraging the mobility of PLA molecular chains; as a consequence a slightly increase in the PLA crystallinity content is registered (Jiang et al., 2006; Arruda et al., 2015; Wang et al., 2018).

A second melting peak due to the presence of the polypropylene in POE-g-GMA is observed for all ternary blends; increasing the POE-g-GMA content this secondary peak is more pronounced.

Effect of Plasticizers on Ternary Blends

On the basis of the mechanical and thermal results showed in the previous section, it emerged that the ternary blend (90-10)+10POE can be chosen as starting point for the final formulation. The choice is justified because it has a high impact resistance value (around 7.2 kJ/m^2), not losing significantly in stiffness and strength at break. In addition, the starting composition (81% wt. PLA, 9% wt. PBAT, 10% wt. POE-g-GMA) allows to remain within the definition of biodegradable material, an important feature for the possible exploitation of this formulation in different sectors. More specifically, this formulation contains a not so high quantity of not biodegradable POE-g-GMA, and the EN 13432 standard is respected.

Nevertheless, in order to further increase the polymers mobility, connected to the improvement of elongation at break without losing the achieved impact resistance, two different types of plasticizers were added (at 10 wt.%) to the (90-10)+10POE formulation. The chosen quantity (10 wt.%) of plasticizer would provide a good balance of the final mechanical properties (good elongation at break and at the same time would likely improve Charpy impact resistance) (Baiardo et al., 2003).

TABLE 5 | Main thermal properties taken from DSC second run for samples heated at 10°C/min.

Blend Name	T_g (°C)	T_{cc} (°C)	$T_{m,peak1}$ (°C)	$T_{m,peak2}$ (°C)	$\Delta H_{m,peak1}$ (J/g)	ΔH_{cc} (J/g)	X_{cc} (%)
PLA	62	118	151	/	23.1	19.9	3.4
PBAT	−36	/	124	/	12.9	/	/
POE-g-GMA	/	/	61	164	27.1	/	/
(95-5)+10POE	61	113	147	/	18.2	12.5	7.2
(95-5)+15POE	61	114	147	164	16.7	10.6	8.2
(95-5)+20POE	61	114	147	165	16.7	10.6	8.6
(90-10)+10POE	61	116	148	166	17.0	13.2	5.1
(90-10)+15POE	61	117	148	166	15.5	10.8	6.7
(90-10)+20POE	61	117	148	166	15.5	9.9	8.4
(90-10-10)+10ATBC	43	98	142	165	17.7	14.7	4.6
(90-10-10)+10EJ	45	99	142	167	17.0	13.7	5.1

When a liquid plasticizer is added, a torque decrement is recorded due to the decrease of melt viscosity (Coltelli et al., 2008). This behavior was confirmed for the plasticized ternary blends for which a torque decrement (below the torque value of the pure rubbers) was registered (**Figure 5**). These results are related to the lubricating effect and enhanced chain mobility that the addition of plasticizers does (Alias and Ismail, 2019). This viscosity decrement was also reflected in the processing conditions: the extrusion temperature profile was decreased of 5°C and also the injection temperature profile was decreased (**Table 2**).

The mechanical tests of the plasticized ternary blend showed very interesting results (**Figure 6** and **Table 3**). In addition to the expected increase in elongation at break, a further increment of Charpy Impact Strength was achieved with the addition of plasticizers. Furthermore, in the tensile tests, a more ductile stress-strain curve was recorded and the materials showed a yielding behavior that was not present in the previous ternary blends. On the other hand, as it can be expected, the plasticizer addition reduces the Elastic Modulus of the final material.

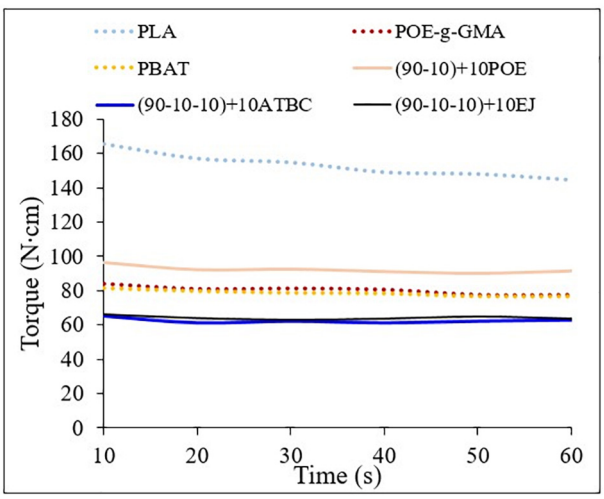

FIGURE 5 | Torque trend for plasticized ternary blends.

The mechanical results showed that EJ-400 reached the best compromise in terms of mechanical properties providing the highest value of Charpy impact resistance (9.1 kJ/m^2), a good value of elongation at break (around 8%) and an acceptable decrement of the Elastic Modulus, thus making this formulation functional for injection molded objects having a good stiffness without losing the flexibility.

To evaluate and deeply understand the effective toughness enhancement of the plasticized ternary blends, the elasto-plastic fracture mechanics approach has been applied to evaluate the J_{Ilim} value (energy absorbed at the moment of the crack

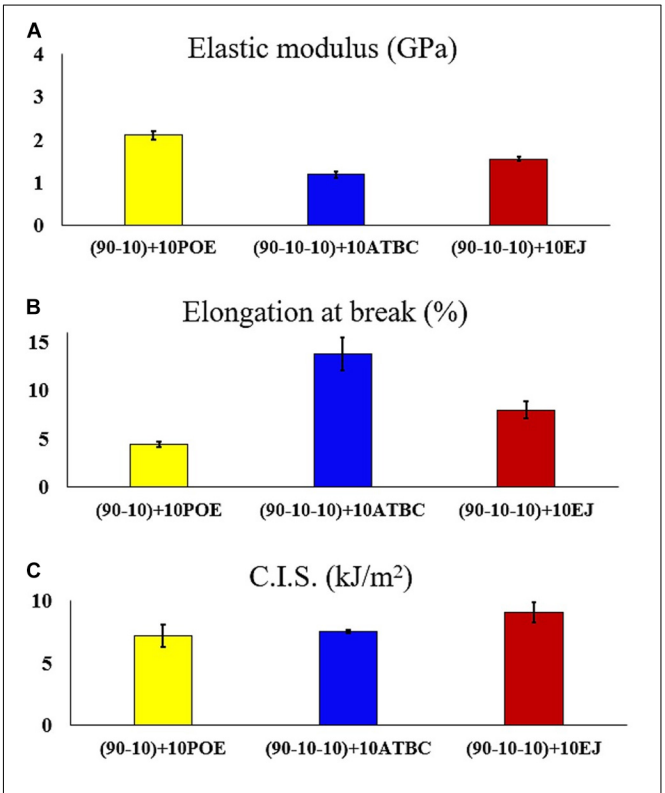

FIGURE 6 | Mechanical properties for plasticized ternary blends: **(A)** Elastic Modulus; **(B)** Elongation at break; **(C)** Charpy Impact Resistance.

propagation during a slow-rate test) and the results are reported in **Figure 7**. For all ternary systems a good J_{Ilim} value was obtained. This value, is very high if compared to the "brittle" G value of PLA found in literature [2.97 kJ/m^2 (Nascimento et al., 2010; Todo and Takayam, 2012)] and also if compared to PLA/PBAT binary blends with 10 wt.% of PBAT (6.5 kJ/m^2 Gigante et al., 2019). The fracture energy released at the beginning of the crack propagation is very impressive both for the plasticized blends and the (90-10)+10POE blend. However, the best J_{Ilim} value (13.6 kJ/m^2) was registered for the blend containing EJ-400 in accordance with the results obtained from quasi-static tensile tests. The improvement in toughness seems to be correlated to the presence of the reactive plasticized system (EJ-400) that would compatibilise the rubber domains within the PLA matrix. This behavior can be explained stating that the epoxy groups of this reactive plasticizer, going to bind with the hydroxyl groups of the PLA, developing a structure that allows the improvement of the ductility of the final blend. The decreasing of energy absorbed from slow rate three-point bending test (1 mm/min) to impact test (4.08 m/s) even if not so evident, is well known in literature (Bucknall et al., 2000; Inberg et al., 2002).

In order to correlate the toughening mechanism to morphology, mechanical results and micromechanical deformation mechanism, dilatometric tests were carried out on these blends. Data of volume change (calculated according

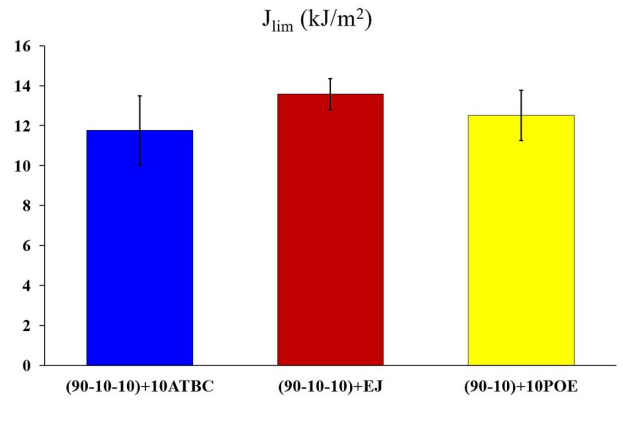

FIGURE 7 | J_{Ilim} values for plasticized ternary blends.

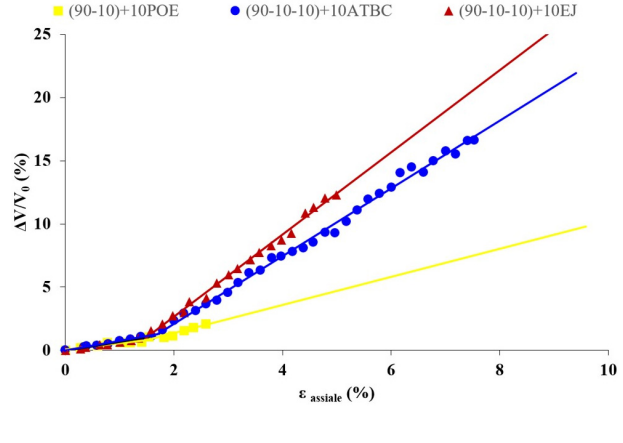

FIGURE 8 | Volume strain vs. longitudinal strain for plasticized ternary.

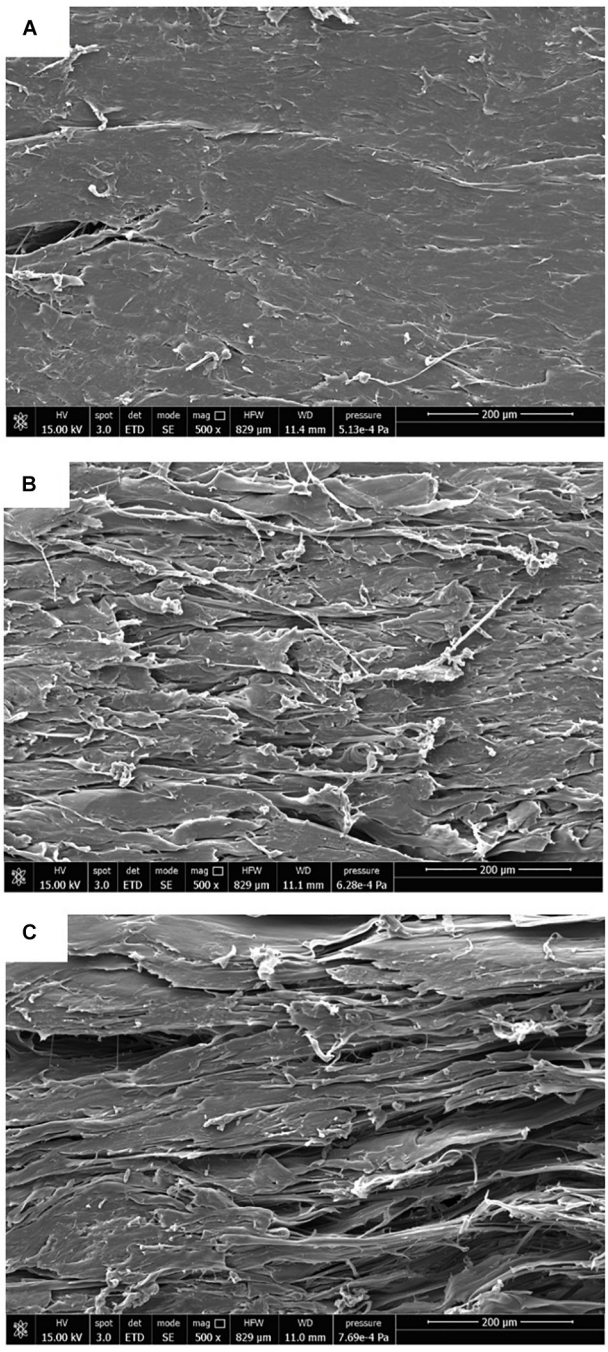

FIGURE 9 | SEM micrographs at the surface of the tensile specimen cryo-fractured along the draw direction for: **(A)** (90-10)+10POE; **(B)** (90-10-10)+10ATBC; **(C)** (90-10-10)+10EJ.

to Equation 1) during tensile tests are shown in **Figure 8** as a function of axial elongation percentage. For the unplasticized (90-10)+10POE ternary system it was not possible to collect data for axial elongation higher than 3% due to the breakage of the specimens.

For the three systems analyzed, different extents of volume increase with increasing of the specimen elongation can be observed. The blend containing EJ-400 exhibits the highest volume increase that it is maintained over the whole range of elongation explored. The blend with ATBC show a similar trend but with a minor volume increment with the axial elongation. These results indicate that the presence of plasticizers in the blend favored dilatation processes that can be related to different micromechanical mechanisms (matrix crazing, debonding of secondary phase particles and cavitation of rubber particles) (Yokoyama and Ricco, 1998). Three different steps are involved during the deformation of rubber-toughened polymers: elastic deformation, plastic strain softening, and strain hardening in yielding zone. Due to stress concentrations around rubber particles, they started to deform and induce cavitation (Alias and Ismail, 2019). The dominant mechanism of micromechanical deformation varies and it is influenced by the chemical structure deformation, the composition of the matrix material, and also by the test temperature, the strain rate and the morphology (shape and size of the rubber particles) (Michler and Bucknall, 2001; Li and Shimizu, 2009).

The point in which the slope change occurs in the volume strain curves (**Figure 8**), detects the longitudinal elongation value for which the cavitation takes place. It can be deduced that the cavitation mechanism starts before the yield point (that for both plasticized ternary blend it is registered around 4% of axial elongation), this behavior was found in literature for other rubber toughened systems (Borggreve and Gaymans, 1988; Lazzeri and Bucknall, 1993, 1995; Yokoyama and Ricco, 1998). At low rates, the volume strain-behavior of the ternary systems analyzed appears to be not so different. The greater difference between the ternary system can be observed at higher rates for which the accelerated voiding process is evident for the plasticized ternary systems. In particular, the ternary blend containing EJ-400 seems to have a more accelerated voiding process. To better understand the data obtained, SEM micrographs at the surface of the specimens, after the uniaxial tensile test, cryo-fractured along the tensile direction were carried out (**Figure 9**). First of all, it can be observed that, differently from the unplasticized ternary blends, many big voids, elongated along the tensile direction, are present. A greater and more extensive voids quantity can be seen for the ternary blend containing EJ-400. This result is in accordance with the dilatometric results for which is higher the slope of the volume strain curve. Also the mechanical results are in accordance. In fact, the Charpy impact resistance is higher for the EJ-400 blend but the elongation at break is lower than the ATBC blend. This is due to the fact that an excessive quantity of void reduces the load bearing section of the sample during the tensile test, triggering a premature specimen breakage.

It has been demonstrated in literature, that EJ-400 is an efficient plasticizer for PLA/rubber systems able to improve the blend compatibility (Mallegni et al., 2018). From the SEM micrographs of (90-10)+10POE ternary blends (**Figure 3**), it can be observed that a more homogeneous dispersed distribution of rubber domains inside the PLA matrix occurred. On the other hand, weak adhesion between the rubber domains and the PLA matrix can be observed for the unplasticized ternary blend.

The thermograms of plasticized ternary blends (shown in **Figure 4D**) exhibits also in this case three main transitions: glass transition, cold crystallization exotherm and melting endotherm. The measured value with relative enthalpies are summarized in **Table 5**. The effect of the plasticizer addition seems not depend from the type of plasticizer used. It is well-known that the plasticizers lower the glass transition temperature (Baiardo et al., 2003). A marked decrement of T_g can be observed for the plasticized ternary blends. This phenomenon influenced the injection molding conditions in fact the mold temperature, set in proximity of T_g, passed from 50°C to 40°C. The incorporation of plasticizers also decreased the cold crystallization temperature by approximately 20°C. However, the addition of POE-g-GMA and also of plasticizers restricts the crystalline ability of PLA as it can be observed from the crystallinity percentage value

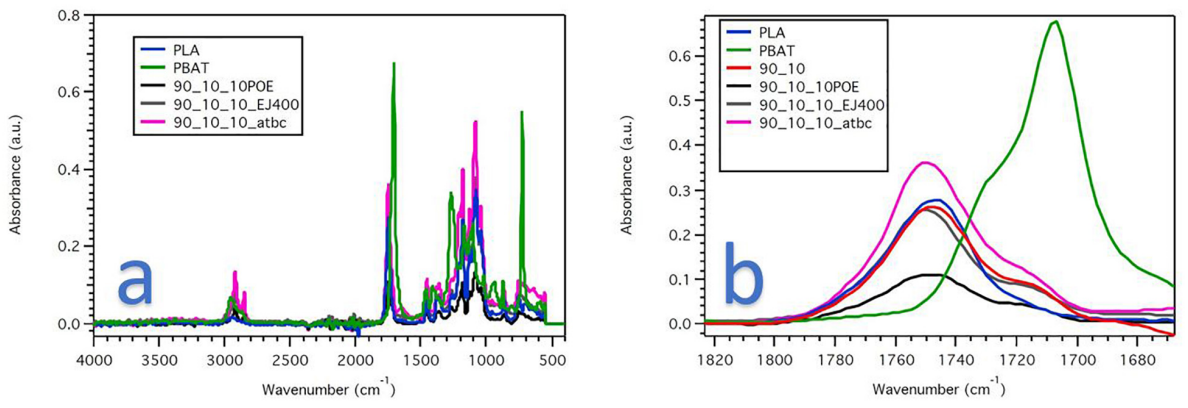

FIGURE 10 | (A) ATR spectra of binary and ternary blends and **(B)** detail of the 1700–1800 cm^{-1} range.

of plasticized ternary compared to the unplasticized one. This behavior was found in literature for a similar system (Zhao et al., 2015). A multiple melting behavior, typical of PLA (Di Lorenzo, 2006; AAliotta et al., 2017) appears for the plasticized blends. This behavior was induced by the presence of plasticizer during the melting process when the unperfected crystals had sufficient time to melt and reorganize into perfect crystals and re-melt at higher temperature (Zhao et al., 2015).

FT-IR spectra of PLA and PBAT were compared to those of the 90/10 blends, containing POE and ATBC or EJ400 (**Figure 10A**). Among other, a strong absorbance peak was detected in the 1700–1800 wavenumber range, attributable to the carbonyl ester C = O stretching of polyesters, both in main chain (PLA and PBAT) as well as in side chains (POE). Noteworthy, the detail of the 1700–1800 wavenumber range (**Figure 10B**) showed a slight shift toward higher wavenumber (1747 cm^{-1}) as a consequence of introduction of POE with respect to pure PLA (1743 cm^{-1}) in 90/10 blends. Remarkably, the introduction of ATBC or EJ400 in 90/10/10 blends further shifted the carbonyl stretching shift to 1751 cm^{-1} (**Figure 10B**). These behaviors suggest that slightly different average dipole distribution around the carbonyl ester groups in PLA occurred as a consequences of the introduction of POE and ATBC or POE and EJ400, confirming the interaction of the PLA matrix with the additives.

CONCLUSIONS

In this study a multiphase ternary system, with two different types of elastomers (PBAT and POE-g-GMA) added in different amounts into a PLA matrix, was investigated and compared with PLA and PLA/PBAT binary blends with maximum 10% wt. of PBAT. The purpose of the present work was to find a compromise in the use of both elastomers (PBAT and POE-g-GMA) as dispersed phases into a PLA matrix to improve impact resistance of PLA using a ternary blend approach without compromising the end of life biodegradability (following the EN 13432 standard). This idea was developed studying many papers in which PBAT caused an improvement in tensile flexibility via direct melt blending with PLA, while POE-g-GMA can increase impact properties.

The work was characterized by a first step in which PLA/PBAT and POE-g-GMA ternary blends were extruded and compared, from the mechanical and thermal point of view, with PLA and binary blends PLA-PBAT. Thanks to an analytical study based on interfacial tensions and morphological considerations, in this screening phase it was found that the two rubber phases stay separated and dispersed in the PLA matrix, evidence confirmed also by SEM analysis. Very good impact properties were achieved for these ternary systems, however, the elongation at break under uniaxial tensile test was not adequate. As a consequence, to the best ternary blend (81 wt.% PLA, 9 wt.% PBAT, and 10 wt.% POE-g-GMA) the effect of plasticizer addition in small amount (10 wt.%) was investigated. Two types of plasticizers were selected: one reactive (EJ-400) and one not reactive (ATBC). Dilatometric tests and the elasto-plastic fracture mechanics were analyzed to clarify the toughening mechanism and also to correlate it with the blends morphology.

It has been demonstrated that the reactive plasticizer EJ-400, improving the compatibility of the rubber domains into the PLA matrix, is a more effective plasticizer. A good balance of tensile results and impact resistance was achieved and confirmed by the J_{Ilim} value and volume strain curves. The best formulation, with the addition of EJ-400, guarantees a useful compromise in terms of mechanical properties providing the highest value of Charpy impact resistance (9.1 kJ/m^2), a good value of elongation at break (around 8%) and an acceptable decrement of the Elastic Modulus with respect to pure PLA and binary blends, making this formulation functional for injection molded PLA based objects and issues that need biodegradability approval, acceptable thermal properties, wide processability window, a good stiffness and, above all, high impact properties (given by a small amount of POE-g-GMA) without losing in terms of elongational flexibility, typical of PBAT.

DATA AVAILABILITY STATEMENT

The original contributions presented in the study are included in the article/supplementary material, further inquiries can be directed to the corresponding author.

AUTHOR CONTRIBUTIONS

LA and VG performed the experimental work and wrote the original draft of the manuscript. AL supervised the study results, the discussion and revised the manuscript. OA contributed to the experimental results. FS performed FT-IR analysis and contributed to the discussion.

ACKNOWLEDGMENTS

Centre for Instrumentation Sharing – University of Pisa (CISUP) is thanked for its support in the use of FEI Quanta 450 FEG scanning electron microscope.

REFERENCES

Agnelli, S., Baldi, F., Castellani, L., Pisoni, K., Vighi, M., and Laiarinandrasana, L. (2018). Study of the plastic deformation behaviour of ductile polymers: use of the material key curves. *Mech. Mater.* 117, 105–115. doi: 10.1016/j.mechmat.2017.11.002

Agnelli, S., Baldi, F., and Riccò, T. (2012). A tentative application of the energy separation principle to the determination of the fracture resistance (JIc) of rubbers. *Eng. Fract. Mech.* 90, 76–88. doi: 10.1016/j.engfracmech.2012.04.020

Alias, N. F., and Ismail, H. (2019). An overview of toughening polylactic acid by an elastomer. *Polym. Technol. Mater.* 58, 1399–1422. doi: 10.1080/25740881.2018.1563118

Aliotta, L., Cinelli, P., Coltelli, M. B., and Lazzeri, A. (2019). Rigid filler toughening in PLA-Calcium Carbonate composites: effect of particle surface treatment and matrix plasticization. *Eur. Polym. J.* 113, 78–88. doi: 10.1016/j.eurpolymj.2018.12.042

Aliotta, L., Cinelli, P., Coltelli, M. B., Righetti, M. C., Gazzano, M., and Lazzeri, A. (2017). Effect of nucleating agents on crystallinity and properties of poly (lactic acid) (PLA). *Eur. Polym. J.* 93, 822–832. doi: 10.1016/j.eurpolymj.2017.04.041

Al-Itry, R., Lamnawar, K., and Maazouz, A. (2012). Improvement of thermal stability, rheological and mechanical properties of PLA. PBAT and their blends by reactive extrusion with functionalized epoxy. *Polym. Degrad. Stab.* 97, 1898–1914. doi: 10.1016/j.polymdegradstab.2012.06.028

Anderson, K. S., and Hillmyer, M. A. (2004). The influence of block copolymer microstructure on the toughness of compatibilized polylactide/polyethylene blends. *Polymer* 45, 8809–8823. doi: 10.1016/j.polymer.2004.10.047

Anderson, K. S., Schreck, K. M., and Hillmyer, M. A. (2008). Toughening Polylactide. *Polym. Rev.* 48, 85–108. doi: 10.1080/15583720701834216

Arruda, L. C., Magaton, M., Bretas, R. E. S., and Ueki, M. M. (2015). Influence of chain extender on mechanical, thermal and morphological properties of blown films of PLA/PBAT blends. *Polym. Test.* 43, 27–37. doi: 10.1016/j.polymertesting.2015.02.005

Baiardo, M., Frisoni, G., Scandola, M., Rimelen, M., Lips, D., Ruffieux, K., et al. (2003). Thermal and mechanical properties of plasticized Poly(L-lactic acid). *J. Appl. Polym. Sci.* 90, 1731–1738. doi: 10.1002/app.12549

Baldi, F., Agnelli, S., and Riccò, T. (2010). On the applicability of the load separation criterion in determining the fracture resistance (JIC) of ductile polymers at low and high loading rates. *Int. J. Fract.* 165, 105–119. doi: 10.1007/s10704-010-9510-9

Baldi, F., Agnelli, S., and Riccò, T. (2013). On the determination of the point of fracture initiation by the load separation criterion in J-testing of ductile polymers. *Polym. Test.* 32, 1326–1333. doi: 10.1016/j.polymertesting.2013.08.007

Barletta, M., and Puopolo, M. (2019). Thermo-mechanical properties of injection molded components manufactured by engineered biodegradable blends. *J. Polym. Environ.* 27, 2105–2118. doi: 10.1007/s10924-019-01500-4

Bernal, C. R., Montemartini, P. E., and Frontini, P. M. (1996). The use of load separation criterion and normalization method in ductile fracture characterization of thermoplastic polymers. *J. Polym. Sci. Part B Polym. Phys.* 34, 1869–1880.

Blackman, B., Baldi, F., Castellani, L., Frontini, P., Laiarinandrasana, L., Pegoretti, A., et al. (2015). Application of the load separation criterion in J-testing of ductile polymers: a round-robin testing exercise. *Polym. Test.* 44, 72–81. doi: 10.1016/j.polymertesting.2015.03.019

Borggreve, R. J. M., and Gaymans, R. J. (1988). Impact modification of poly(caprolactam) by copolymerization with a low molecular weight polybutadiene. *Polymer* 29, 1441–1446. doi: 10.1016/0032-3861(88)90308-4

Bucknall, C. B., Heather, P. S., and Lazzeri, A. (2000). Rubber toughening of plastics. *J. Mater. Sci.* 24, 2255–2261. doi: 10.1007/BF02385450

Cao, X., Mohamed, A., Gordon, S. H., Willett, J. L., and Sessa, D. J. (2003). DSC study of biodegradable poly(lactic acid) and poly(hydroxy ester ether) blends. *Thermochim. Acta* 406, 115–127. doi: 10.1016/S0040-6031(03)00252-1

Cinelli, P., Seggiani, M., Mallegni, N., Gigante, V., and Lazzeri, A. (2019). Processability and degradability of PHA-based composites in terrestrial environments. *Int. J. Mol. Sci.* 20:284. doi: 10.3390/ijms20020284

Coltelli, M. B., Della Maggiore, I., Bertoldo, M., Signori, F., Bronco, S., and Ciardelli, F. (2008). Poly(lactic acid) properties as a consequence of poly(butylene adipate-co-terephthalate) blending and acetyl tributyl citrate plasticization. *J. Appl. Polym. Sci.* 110, 1250–1262. doi: 10.1002/app.28512

Dekkers, M. E. J., Hobbs, S. Y., and Watkins, V. H. (1991). Morphology and deformation behaviour of toughened blends of poly(butylene terephthalate), polycarbonate and poly(phenylene ether). *Polymer* 32, 2150–2154. doi: 10.1016/0032-3861(91)90039-L

Di Lorenzo, M. L. (2006). Calorimetric analysis of the multiple melting behavior of poly(L-lactic acid). *J. Appl. Polym. Sci.* 100, 3145–3151. doi: 10.1002/app.23136

European Committee for Standardisation (1999). *EN 13432. Requirements for Packaging Recoverable through Composting and Biodegradation–Test Scheme and Evaluation Criteria for the Final Acceptance of Packaging.* Brussels: European Committee for Standardisation.

Forghani, E., Azizi, H., Karabi, M., and Ghasemi, I. (2018). Compatibility, morphology and mechanical properties of polylactic acid/polyolefin elastomer foams. *J. Cell. Plast.* 54, 235–255. doi: 10.1177/0021955X16681450

Gigante, V., Canesi, I., Cinelli, P., Coltelli, M., and Lazzeri, A. (2019). Rubber toughening of Polylactic acid (PLA) with Poly(butylene adipate-co-terephthalate) (PBAT): mechanical properties, fracture mechanics and analysis of brittle – ductile behavior while varying temperature and test speed. *Eur. Polym. J.* 115, 125–137. doi: 10.1016/j.eurpolymj.2019.03.015

Grande, R., and Carvalho, A. J. F. (2011). Compatible ternary blends of chitosan/poly(vinyl alcohol)/poly(lactic acid) produced by oil-in-water emulsion processing. *Biomacromolecules* 12, 907–914. doi: 10.1021/bm101227q

Gross, R. A., and Kalra, B. (2002). Biodegradable polymers for the environment. *Science* 297, 803–807. doi: 10.1126/science.297.5582.803

Gu, S. Y., Zhang, K., Ren, J., and Zhan, H. (2008). Melt rheology of polylactide/poly(butylene adipate-co-terephthalate) blends. *Carbohydr. Polym.* 74, 79–85. doi: 10.1016/j.carbpol.2008.01.017

Gupta, A. K., and Srinivasan, K. R. (1993). Melt rheology and morphology of PP/SEBS/PC ternary blend. *J. Appl. Polym. Sci.* 47, 167–184.

Hamad, K., Kaseem, M., Ayyoob, M., Joo, J., and Deri, F. (2018). Polylactic acid blends: the future of green, light and tough. *Prog. Polym. Sci.* 85, 83–127. doi: 10.1016/j.progpolymsci.2018.07.001

Hemmati, M., Nazokdast, H., and Panahi, H. S. (2001). Study on morphology of ternary polymer blends. I. Effects of melt viscosity and interfacial interaction. *J. Appl. Polym. Sci.* 82, 1129–1137. doi: 10.1002/app.1947

Hu, G., Sun, Y., and Lambla, M. (1996). Effects of processing parameters on the in situ compatibilization of polypropylene and poly (butylene terephthalate) blends by one-step reactive extrusion. *J. Appl. Polym. Sci.* 61, 1039–1047.

Inberg, J. P. F., Takens, A., and Gaymans, R. J. (2002). Strain rate effects in polycarbonate and polycarbonate/ABS blends. *Polymer* 43, 2795–2802. doi: 10.1016/S0032-3861(02)00081-2

Ishida, S., Nagasaki, R., Chino, K., Dong, T., and Inoue, Y. (2009). Toughening of Poly(L-lactide) by Melt Blending with Rubbers. *J. Appl. Polym. Sci.* 559–566. doi: 10.1002/app.30134

Jiang, L., Wolcott, M. P., and Zhang, J. (2006). Study of biodegradable polylactide/poly(butylene adipate-co-terephthalate) blends. *Biomacromolecules* 7, 199–207. doi: 10.1021/bm050581q

Kumar, M., Mohanty, S., Nayak, S. K., and Rahail Parvaiz, M. (2010). Effect of glycidyl methacrylate (GMA) on the thermal, mechanical and morphological property of biodegradable PLA/PBAT blend and its nanocomposites. *Bioresour. Technol.* 101, 8406–8415. doi: 10.1016/j.biortech.2010.05.075

Künkel, A., Becker, J., Börger, L., Hamprecht, J., Koltzenburg, S., Loos, R., et al. (2016). "Polymers, Biodegradable," in *Ullmann's Encyclopedia of Industrial Chemistry Major Reference Works*, 1–29. doi: 10.1002/14356007.n21_n01.pub2

Kunthadong, P., Molloy, R., Worajittiphon, P., Leejarkpai, T., Kaabbuathong, N., and Punyodom, W. (2015). Biodegradable plasticized blends of Poly(L-lactide) and cellulose acetate butyrate: from blend preparation to biodegradability in real composting conditions. *J. Polym. Environ.* 23, 107–113. doi: 10.1007/s10924-014-0671-x

La Mantia, F. P., Morreale, M., Botta, L., Mistretta, M. C., Ceraulo, M., and Scaffaro, R. (2017). Degradation of polymer blends: a brief review. *Polym. Degrad. Stab.* 145, 79–92. doi: 10.1016/j.polymdegradstab.2017.07.011

Lazzeri, A., and Bucknall, C. B. (1993). Dilatational bands in rubber-toughened polymers. *J. Mater. Sci.* 28, 6799–6808. doi: 10.1007/BF00356433

Lazzeri, A., and Bucknall, C. B. (1995). Applications of a dilatational yielding model to rubber-toughened polymers. *Polymer* 36, 2895–2902. doi: 10.1016/0032-3861(95)94338-T

Lazzeri, A., Thio, Y. S., and Cohen, R. E. (2004). Volume strain measurements on CACO3/polypropylene particulate composites: the effect of particle size. *J. Appl. Polym. Sci.* 91, 925–935. doi: 10.1002/app.13268

Li, Y., and Shimizu, H. (2009). Improvement in toughness of poly (l-lactide)(PLLA) through reactive blending with acrylonitrile–butadiene–styrene copolymer (ABS): morphology and properties. *Eur. Polym. J.* 45, 738–746. doi: 10.1016/j.eurpolymj.2008.12.010

Luzinov, I., Xi, K., Pagnoulle, C., Huynh-Ba, G., and Jérôme, R. (1999). Composition effect on the core–shell morphology and mechanical properties of ternary polystyrene/styrene–butadiene rubber/polyethylene blends. *Polymer* 40, 2511–2520.

Maiza, M., Benaniba, M. T., and Massardier-Nageotte, V. (2016). Plasticizing effects of citrate esters on properties of poly(lactic acid). *J. Polym. Eng.* 36, 371–380. doi: 10.1515/polyeng-2015-0140

Mallegni, N., Phuong, T. V., Coltelli, M. B., Cinelli, P., and Lazzeri, A. (2018). Poly(lactic acid) (PLA) based tear resistant and biodegradable flexible films by blown film extrusion. *Materials* 11:148. doi: 10.3390/ma11010148

Michler, G. H., and Bucknall, C. B. (2001). New toughening mechanisms in rubber modified polymers. *Plast. Rubber Compos.* 30, 110–115. doi: 10.1179/146580101101541516

Murariu, M., and Dubois, P. (2016). PLA composites: from production to properties. *Adv. Drug Deliv. Rev.* 107, 17–46. doi: 10.1016/j.addr.2016.04.003

Nagarajan, V., Mohanty, A. K., and Misra, M. (2018). Blends of polylactic acid with thermoplastic copolyester elastomer: effect of functionalized terpolymer type on reactive toughening. *Polym. Eng. Sci.* 58, 280–290. doi: 10.1002/pen.24566

Nascimento, L., Gamez-Perez, J., Santana, O. O., Velasco, J. I., Maspoch, M. L., and Franco-Urquiza, E. (2010). Effect of the recycling and annealing on the mechanical and fracture properties of Poly(Lactic Acid). *J. Polym. Environ.* 18, 654–660. doi: 10.1007/s10924-010-02295

Nofar, M., Maani, A., Sojoudi, H., Heuzey, M. C., and Carreau, P. J. (2015). Interfacial and rheological properties of PLA/PBAT and PLA/PBSA blends and their morphological stability under shear flow. *J. Rheol.* 59, 317–333. doi: 10.1122/1.4905714

Phuong, V. T., Coltelli, M.-B., Cinelli, P., Cifelli, M., Verstichel, S., and Lazzeri, A. (2014). Compatibilization and property enhancement of poly(lactic acid)/polycarbonate blends through triacetin-mediated interchange reactions in the melt. *Polymer* 55, 4498–4513. doi: 10.1016/j.polymer.2014.06.070

Plackett, D., Andersen, T. L., Pedersen, W. B., and Nielsen, L. (2003). Biodegradable composites based on L-polylactide and jute fibres. *Compos. Sci. Technol.* 63, 1287–1296. doi: 10.1016/S0266-3538(03)00100-3

Platt, D. K. (2006). *Biodegradable Polymers: Market Report*. London: iSmithers Rapra Publishing.

Quero, E., Müller, A. J., Signori, F., Coltelli, M. B., and Bronco, S. (2012). Isothermal cold-crystallization of PLA/PBAT blends with and without the addition of acetyl tributyl citrate. *Macromol. Chem. Phys.* 213, 36–48. doi: 10.1002/macp.201100437

Ren, J., Fu, H., Ren, T., and Yuan, W. (2009). Preparation, characterization and properties of binary and ternary blends with thermoplastic starch, poly(lactic acid) and poly(butylene adipate-co-terephthalate). *Carbohydr. Polym.* 77, 576–582. doi: 10.1016/j.carbpol.2009.01.024

Sarazin, P., Li, G., Orts, W. J., and Favis, B. D. (2008). Binary and ternary blends of polylactide, polycaprolactone and thermoplastic starch. *Polymer* 49, 599–609. doi: 10.1016/j.polymer.2007.11.029

Sedničková, M., Pekaøová, S., Kucharczyk, P., Bočkaj, J., Janigová, I., Kleinová, A., et al. (2018). Changes of physical properties of PLA-based blends during early stage of biodegradation in compost. *Int. J. Biol. Macromol.* 113, 434–442. doi: 10.1016/j.ijbiomac.2018.02.078

Sharobeam, M. H., and Landes, J. D. (1991). The load separation criterion and methodology in ductile fracture mechanics. *Int. J. Fract.* 47, 81–104. doi: 10.1007/BF00032571

Signori, F., Coltelli, M. B., and Bronco, S. (2009). Thermal degradation of poly(lactic acid) (PLA) and poly(butylene adipate-co-terephthalate) (PBAT) and their blends upon melt processing. *Polym. Degrad. Stab.* 94, 74–82. doi: 10.1016/j.polymdegradstab.2008.10.004

Su, Z., Li, Q., Liu, Y., Hu, G. H., and Wu, C. (2009). Compatibility and phase structure of binary blends of poly(lactic acid) and glycidyl methacrylate grafted poly(ethylene octane). *Eur. Polym. J.* 45, 2428–2433. doi: 10.1016/j.eurpolymj.2009.04.028

Sun, S., Zhang, M., Zhang, H., and Zhang, X. (2011). Polylactide toughening with epoxy-functionalized grafted acrylonitrile–butadiene–styrene particles. *J. Appl. Polym. Sci.* 122, 2992–2999.

Svoboda, P., Theravalappil, R., Svoboda, D., Mokrejs, P., Kolomaznik, K., Mori, K., et al. (2010). Elastic properties of polypropylen/ethylene-octene copolymer blends. *Polym. Test.* 29, 742–748. doi: 10.1016/j.polymertesting.2010.05.014

Todo, M., and Takayam, T. (2012). "Fracture mechanisms of biodegradable PLA and PLA/PCL blends," in *Biomaterials-Physics and Chemistry*, ed. R. Pignatello (London: IntechOpen), doi: 10.5772/24199

Utracki, L. A., and Shi, Z. H. (1992). Development of polymer blend morphology during compounding in a twin-screw extruder. Part I: droplet dispersion and coalescence—a review. *Polym. Eng. Sci.* 32, 1824–1833. doi: 10.1002/pen.760322405

Wang, X., Mi, J., Wang, J., Zhou, H., and Wang, X. (2018). Multiple actions of poly(ethylene octene) grafted with glycidyl methacrylate on the performance of poly(lactic acid). *RSC Adv.* 8, 34418–34427. doi: 10.1039/C8RA07510G

Wu, S. (1985). Phase structure and adhesion in polymer blends: a criterion for rubber toughening. *Polymer* 26, 1855–1863. doi: 10.1016/0032-3861(85)90015-1

Xue, B., He, H., Zhu, Z., Li, J., Huang, Z., Wang, G., et al. (2018). A Facile fabrication of high toughness poly(lactic acid) via reactive extrusion with poly(butylene succinate) and ethylene-methyl acrylate-glycidyl methacrylate. *Polymers* 10, 1–15. doi: 10.3390/polym10121401

Yeh, J., Tsou, C., Huang, C., Chen, K., and Wu, C. (2009). Compatible and Crystallization Properties of Poly (lactic acid)/ Poly (butylene adipate- co -terephthalate) Blends. *J. Appl. Polym. Sci.* 116, 680–687. doi: 10.1002/app

Yokoyama, Y., and Ricco, T. (1998). Toughening of polypropylene by different elastomeric systems. *Polymer* 39, 3675–3681. doi: 10.1016/S0032-3861(97)10358-5

Zhang, K., Nagarajan, V., Misra, M., and Mohanty, A. K. (2014). Supertoughened renewable PLA reactive multiphase blends system: phase morphology and performance. *ACS Appl. Mater. Interfaces* 6, 12436–12448. doi: 10.1021/am502337u

Zhang, N., Wang, Q., Ren, J., and Wang, L. (2009). Preparation and properties of biodegradable poly(lactic acid)/poly(butylene adipate-co-terephthalate) blend with glycidyl methacrylate as reactive processing agent. *J. Mater. Sci.* 44, 250–256. doi: 10.1007/s10853-008-3049-4

Zhao, Y., Lang, X., Pan, H., Wang, Y., Yang, H., Zhang, H., et al. (2015). Effect of mixing poly(lactic acid) with glycidyl methacrylate grafted poly(ethylene octene) on optical and mechanical properties of the blown films. *Polym. Eng. Sci.* 55, 2801–2813. doi: 10.1002/pen.24171

Conflict of Interest: The authors declare that the research was conducted in the absence of any commercial or financial relationships that could be construed as a potential conflict of interest.